Atmos. Chem. Phys. Discuss., https://doi.org/10.5194/acp-2019-354
Manuscript under review for journal Atmos. Chem. Phys.
Discussion started: 25 April 2019

Atmospheric Chemistry and Physics Discussions

Ozone formation under low solar radiation in eastern China

Xuexi Tie[1,2], Xin Long[1], Guohui Li[1], Shuyu Zhao[1], Jianming Xu[3,4]

[1] KLACP, SKLLQG, Institute of Earth Environment, Chinese Academy of Sciences, Xi'an 710061, China

[2]Center for Excellence in Urban Atmospheric Environment, Institute of Urban Environment, Chinese Academy of Sciences, Xiamen 361021, China

[3] Shanghai Meteorological Service, Shanghai, 200030, China

[4]Shanghai Key Laboratory of Meteorology and Health, Shanghai, 200030, China

Correspondence to: XueXi Tie (tiexx@ieecas.cn) or
Jianming Xu (metxujm@163.cn)

Atmos. Chem. Phys. Discuss., https://doi.org/10.5194/acp-2019-354
Manuscript under review for journal Atmos. Chem. Phys.
Discussion started: 25 April 2019

Atmospheric Chemistry and Physics Discussions

Abstract

$PM_{2.5}$, a particulate matter with a diameter of 2.5 micrometers or less, is one of the major components of the air pollution in eastern China. In the past few years, China's government made strong efforts to reduce the $PM_{2.5}$ pollutions. However, another important pollutant (ozone) becomes an important problem in eastern China. Ozone (O_3) is produced by photochemistry, which requires solar radiation for the formation of O_3. Under heavy $PM_{2.5}$ pollution, the solar radiation is often depressed, and the photochemical production of O_3 is prohibited. This study shows that during fall in eastern China, under heavy $PM_{2.5}$ pollutions, there were often strong O_3 photochemical productions, causing a co-occurrence of high $PM_{2.5}$ and O_3 concentrations. This co-occurrence of high $PM_{2.5}$ and O_3 is un-usual and is the main focus of this study. Recent measurements show that there were often high HONO surface concentrations in major Chinese mega cities, especially during daytime, with maximum concentrations ranging from 0.5 to 2 ppbv. It is also interesting to note that the high HONO concentrations were occurred during high aerosol concentration periods, suggesting that there were additional HONO surface sources in eastern China. Under the high daytime HONO concentrations, HONO can be photo-dissociated to be OH radicals, which enhance the photochemical production of O_3. In order to study the above scientific issues, a radiative transfer model (TUV; Tropospheric Ultraviolet-Visible) is used in this study, and a chemical steady state model is established to calculate OH radical concentrations. The calculations show that by including the OH production of the photo-dissociated of HONO, the calculated OH concentrations are significantly higher than the values without including this production. For example, by including HONO production, the maximum of OH concentration under the high aerosol condition (AOD=2.5) is similar to the value under low aerosol condition (AOD=0.25) in the no-HONO case. This result suggests that even under the high aerosol condition, the chemical oxidizing process for O_3 production can occurred, which explain the co-occurrence of high $PM_{2.5}$ and high O_3 in fall season in eastern China. However, the O_3 concentrations were not significantly

affected by the appearance of HONO in winter. This study shows that the seasonal variation of solar radiation plays important roles for controlling the OH production in winter. When the solar radiation is in a very low level in winter, it reaches the threshold level to prevent the OH chemical production, even by including the HONO production of OH. This study provides some important scientific highlights to better understand the O_3 pollutions in eastern China.

Keywords; High $PM_{2.5}$ and O_3, eastern China, HONO photolysis

Atmos. Chem. Phys. Discuss., https://doi.org/10.5194/acp-2019-354
Manuscript under review for journal Atmos. Chem. Phys.
Discussion started: 25 April 2019

1. Introduction

Currently, China is undergoing a rapid economic development, resulting in a higher demand for energy and greater use of fossil fuels. As a result, the high emissions of pollutants produce heavy pollutions in mega cities of eastern China, such as Beijing and Shanghai. For example, in the city of Shanghai (a largest mega city in China), the urban and economical developments of the city are very rapid. During 1990 to 2015, the population increased from 13.3 to 24.1 million. The number of automobiles increased from 0.2 million (1993) to 2.0 million (2011). The rapid growing population and energy usage caused a rapid increase in the emissions of pollutants, leading to severe air pollution problems in these mega cities (Zhang et al., 2006; Geng et al., 2007; Deng et al., 2008).

Measurements, such as satellite observations have revealed much higher aerosol pollution in eastern China than in eastern US (Tie et al., 2006). The high aerosol pollution causes a wide range of environmental consequences. According to a study by Tie et al. (2009a), exposure to extremely high particle concentrations leads to a great increase of lung cancer cases. High PM (particular matter) concentrations also significantly reduce the range of visibility in China's mega cities (Deng et al., 2008). According to a recent study, the high aerosol pollution causes important effects on the crop (rice and wheat) production in eastern China (Tie et al., 2016).

In the troposphere, ozone formation is resulted from a complicated chemical process, and requires ozone precursors, such as VOCs (volatile organic carbons) and NO_X = $NO + NO_2$ (nitrogen oxides) (Sillman, 1995). As the increase in industrial activity and number of automobiles, the precursors of ozone (O_3) and the global budget of oxidization are also significantly increased (Huang et al., 2017; Huang et al., 2018). As a result, O_3 pollutions are becomes a serous pollution problem in Shanghai and other Chinese mega cities (Geng et al., 2010; Tie 2009b; Tie et al., 2015). The effects on O_3 production rate can be characterized as either NO_X-sensitive or VOC-sensitive conditions (Sillman, 1995; Zhang et al., 2003; Lei et al., 2004; Tie et al., 2013). Thus, better understanding the trends of O_3 precursors (VOCs, NO_X) is important to

99 determine the O_3 trends in Shanghai (as well as many large cities in China).

100 In the past few years, China's government made strong efforts to reduce the $PM_{2.5}$
101 pollutions. However, another important pollutant (O_3) becomes an important problem
102 in eastern China. Several studies regarding the O_3 formation are previously studied in
103 Shanghai. For example, Geng et al. (2007; 2008) study the relationship between O_3
104 precursors (NOx and VOCs) for the ozone formation in Shanghai. Tie et al. (2009)
105 study the short-term variability of O_3 in Shanghai. Their study suggested that in
106 addition to the ozone precursors, meteorological conditions, such as regional transport,
107 have also strong impacts on the ozone concentrations. During September 2009, a
108 major field experiment (the MIRAGE-Shanghai) was conducted in Shanghai, and
109 multiply chemical species were measured during the experiment. The summary of the
110 measurements by Tie et al (2013) suggests that the ozone formation in Shanghai is
111 under VOC-sensitive condition. However, if the emission ration of NOx/VOCs
112 reduces to a lower value (0.1-0.2), the ozone formation in Shanghai will switch from
113 VOC-sensitive condition to NOx-sensitive condition.

114 Despite of some progresses have been made for the ozone formation in mega cities in
115 China, it is still lack of study of ozone development in large cities of China. For
116 example, this study shows that during fall in eastern China, under heavy $PM_{2.5}$
117 pollutions, there were often strong O_3 chemical productions, causing the
118 co-occurrence of high $PM_{2.5}$ and O_3 concentrations. Under heavy aerosol condition,
119 the solar radiation is depressed, significantly reducing the photochemical production
120 of O_3. This co-occurrence of high $PM_{2.5}$ and O_3 is an unusual and is the focus of this
121 study. Recent measurements show that there were often high HONO concentrations in
122 major Chinese mega cities, especially during daytime, with maximum concentrations
123 ranging from 0.5 to 2 ppbv (Huang et al., 2017). It is also interesting to note that the
124 high HONO surface concentrations were occurred during high aerosol concentration
125 periods, suggesting that there are additional HONO surface sources in eastern China.
126 Under the high daytime HONO concentrations, HONO can be photo-dissociated to be
127 OH radicals, which enhance the photochemical production of O_3.

Atmos. Chem. Phys. Discuss., https://doi.org/10.5194/acp-2019-354
Manuscript under review for journal Atmos. Chem. Phys.
Discussion started: 25 April 2019

128

129 The paper is organized as follows: in Section 2, we describe the measurement of O3
130 and PM2.5. In Section 3, we describe the calculation of photo-dissociated rate of
131 HONO and a steady state model for the calculation of OH, and the causes of high O3
132 production under the heavy aerosol condition. Section 4 shows a brief conclusion of
133 the results.

134

135 ## 2. Measurements of O_3 and $PM_{2.5}$

136

137 There are long-term measurements in Eastern China by Chinese Environment
138 Protection Agency (CEPA) for monitoring the air quality in China. In eastern China,
139 especially in the capital city of China (Beijing), there are often heavy air pollutions,
140 especially for fine particular matter ($PM_{2.5}$ – the radium of particle being less than 2.5
141 um). Figure 1 shows the measurement sites in Beijing, in which the measured
142 concentrations of $PM_{2.5}$ and O_3 are used to the analysis. In the region, the air
143 pollutions were very heavy, especially in winter (Long et al., 2016; Tie et al., 2017).
144 The previous studies suggested that the both aerosol and O_3 pollutions became the
145 major pollutants in the region (Li et al., 2017).

146

147 Figure 2 shows the daily averaged concentrations of $PM_{2.5}$ and O_3 in the Beijing
148 region in 2015. The daily averaged concentrations show that there were strong daily
149 and seasonal variations for both the concentrations of $PM_{2.5}$ and O_3. Despite the daily
150 variation, the concentrations of $PM_{2.5}$ existed a strong seasonal variation. For example,
151 there were very high concentrations during winter, with maximum of ~300 $\mu g/m^3$.
152 While in summer, the maximum concentrations reduced to ~150 $\mu g/m^3$. The seasonal
153 variability of O_3 concentrations were opposite with the $PM_{2.5}$ concentrations, with
154 lower concentrations in winter (< 50 μg /m^3) and higher concentrations in summer (>
155 150 $\mu g/m^3$). These seasonal variations of $PM_{2.5}$ and O_3 have been studied by previous
156 studies (Tie and Cao, 2017; Li et al., 2017). Their results suggest that the winter high

157 $PM_{2.5}$ concentrations were resulted from the combination of both the high emissions
158 (heating season in the Beijing region), and poor meteorological ventilation conditions,
159 such as lower PBL (Planetary Boundary Layer) height (Quan et al., 2013; Tie et al.
160 2015). According to the photochemical theory of O_3 formation, the summer high and
161 winter low O_3 concentrations are mainly due to seasonal variation of the solar
162 radiation (Seinfeld, J. H. and Pandis, 2006).
163
164 In addition to the seasonal variation of solar radiation, the heavy aerosol
165 concentrations play important roles to reduce solar radiation, causing the reduction of
166 solar radiation and O_3 formation (Bian et al., 2007). As we show in Fig. 3a, during
167 wintertime, the O_3 concentrations were strong anti-correlated with the $PM_{2.5}$
168 concentrations, suggesting that the reduction of solar radiation by aerosol particles
169 have important impact on the reduction of O_3 concentrations. Figure 3a also shows
170 that the relationship between O_3 and $PM_{2.5}$ was not linearly related. For example,
171 when the concentrations of $PM_{2.5}$ were less than 100 $\mu g/m^3$, O_3 concentrations rapidly
172 decreased with the increase of $PM_{2.5}$ concentrations. In contrast, when the
173 concentrations of $PM_{2.5}$ were greater than 100 $\mu g/m^3$, O_3 concentrations slowly
174 decreased with the increase of $PM_{2.5}$ concentrations. This is consistent with the result
175 of Bian et al (2007).
176
177 It is interesting to note that during late spring, summer, and early fall periods, the
178 correlation between $PM_{2.5}$ and O_3 concentrations was positive relationship compared
179 to the negative relationship in winter (see Fig. 3b). This result suggests that O_3
180 production was high during the heavy haze period, despite the solar radiation was
181 greatly depressed. In order to clearly display this unusual event, we illustrate diurnal
182 variations of $PM_{2.5}$ and O_3, and NO_2 during a fall period (from Oct.5 to Oc. 6, 2015).
183 Figure 4 shows that during this period, the $PM_{2.5}$ concentrations were very high,
184 ranging from 150 to 320 $\mu g/m^3$. Under such high aerosol condition, the solar radiation
185 should be significantly reduced, and O_3 photochemical production would be reduced.
186 However, the diurnal variation of O_3 was unexpectedly strong, with high noontime

187 concentration of >220 $\mu g/m^3$ and very low nighttime concentration of ~25 $\mu g/m^3$. This
188 strong diurnal variation was due to the photochemical activity, which suggested that
189 during relatively low solar conditions, the photochemical activities of O_3 production
190 was high. According to the theory of the O_3 chemical production, the high O_3
191 production is related to high oxidant of OH (Seinfeld and Pandis, 2006), which should
192 not be occurred during lower solar radiation. This result brings important issue for air
193 pollution control strategy, because the both air pollutants (high $PM_{2.5}$ and O_3) were
194 important air pollution problems in eastern China.
195

196 ## 2. Method

197
198 In order to better understand the O_3 chemical production occurred in heavy aerosol
199 condition in eastern Chine, the possible O3 production in such condition is discussed.
200 Ozone photochemical production ($P[O_3]$) is strongly related to the amount of OH
201 radicals (OH) (Chameides et al., 1999). According to the traditional theory, the
202 amount of surface OH radicals is proportional to the surface of solar radiation, which
203 is represented by
204
205 $$[OH] = P[HOx]/L[HOx]^* \quad \text{(R-1)}$$
206
207 Where [OH] represents the concentration of hydroxyl radicals (#/cm^3); HOx
208 represents the concentration of HO_2 + OH (#/cm^3); P[HOx] represents the
209 photochemical production of HOx (#/cm^3/s); and L[HOx]* (1/s) represents the
210 photochemical destruction of HOx, which is normalized by the concentrations of OH.
211
212 The major process for the photochemical production of P[HOx] is through the O_3
213 photolysis and follows by the reaction with atmospheric water vapor. It can express
214 by
215 $$P[HOx] = J_1[O_3]/(k_1 \times am) \times 2.0 \times k_2[H_2O] = P_1[HOx] \quad \text{(R-2)}$$
216

Where J_1 represents the photolysis of $O_3 + h\nu \rightarrow O^1D$; k_1 represents the reaction rate of $O^1D + am \rightarrow O^3P$; and k_2 represents the reaction rate of $O^1D + H_2O \rightarrow 2OH$. As we can see, this HOx production is proportional to the magnitude of solar radiation (J_1), and J_1 is the O_3 photolysis with the solar radiation. Figure 5 shows the relationship between the values of J_1 and aerosol concentrations in October at middle-latitude calculated by the TUV model Madronich and Flocke (1999). This result suggests that under the high aerosol concentrations (AOD = 2.5), the J_1 value is strongly depressed, resulting in significant reduction of OH concentrations and O_3 production. For example, the maximum J_1 value is about $2.7x10^{-5}$ (1/s) with lower aerosol values (AOD = 0.25). According to the previous study, the surface $PM_{2.5}$ concentrations were generally smaller than 50 $\mu g/m^3$ with this AOD value (Tie et al., 2017). However, when the AOD value increase to 2.5 (the $PM_{2.5}$ concentrations are generally >100 $\mu g/m^3$), the maximum J_1 value rapidly decreases to about $6x10^{-6}$ (1/s), which is about 450% reduction compared to the value with AOD=0.25. This study suggests that under high $PM_{2.5}$ concentrations (>100 $\mu g/m^3$), the photochemical production of OH (P[HOx]) is rapidly decreased, leading to low OH concentrations, which cannot initiate the high oxidation of O_3 production. As a result, the high O_3 production shown in Fig. 4 cannot be explained. Other sources for O_3 oxidation are needed to explain this result.

Recent studies show that the HONO concentrations are high in eastern China (Huang et al., 2017). Because under high solar radiation, the photolysis rate of HONO is very high, resulting in very low HONO concentrations in daytime (Seinfeld and Pandis, 2006). These measured high HONO concentrations are explained by their studies. One of the explanations is that there are high surface HONO sources during daytime, which produces high HONO concentrations (Huang et al., 2017).

Figure 6 shows the measured HONO concentrations in two large cities in China (Shanghai and Xi'an) during fall time. It shows that the measured HONO concentrations were high, with a maximum concentration of 2.3 ppbv during morning,

Atmos. Chem. Phys. Discuss., https://doi.org/10.5194/acp-2019-354
Manuscript under review for journal Atmos. Chem. Phys.
Discussion started: 25 April 2019

Atmospheric Chemistry and Physics Discussions

and about 0.5-1.0 ppbv in daytime. It is also interesting to note that the high HONO concentrations were occurred during high aerosol concentration periods. Figure 7 illustrates that when the $PM_{2.5}$ concentrations increased to 70-80 $\mu g/m^3$, and the HONO concentrations enhanced to 1.4-18 ppbv during September in Shanghai. This measured high HONO concentrations were significantly higher than the calculated concentrations (shown in Fig. 6), suggesting that some additional sources of HONO are needed. This result is consistent with the HONO measurements in other Chinese cities (Huang et al. 2017).

Under the high HONO concentrations in daytime, HONO can be photolyzed to be OH, and become another important process to produce OH. As a result, the OH production rate (P[HOx]) can be written to the following reactions.

$$P_2[HOx] = J_2 \times [HONO] \quad \text{(R-3)}$$

$$P[HOx] = P_1[HOx] + P_2[HOx]$$
$$= J_1[O_3]/(k_1 \times am) \times 2.0 \times k_2[H_2O] + J_2 \times [HONO] \quad \text{(R-4)}$$

Because the chemical lifetime of OH is less than second, OH concentrations can be calculated according to equilibrium of chemical production and chemical loss. With the both OH chemical production processes, the OH concentrations can be calculated by the following equation (Seinfeld and Pandis, 2006).

$$P1 + P2 = L1 + L2$$

Where P1 and P2 are the major chemical productions, expressed in R-4, and L1 and L2 are the major chemical loss of OH, and represent by

$$L1: \quad OH + NO_2 \rightarrow HNO_3 \quad \text{(R-5)}$$

$$L2: \quad HO_2 + HO_2 \rightarrow H_2O_2 + O_2 \quad \text{(R-6)}$$

Under high NOx condition, such as in the Shanghai region, NOx concentrations were often higher to 50 ppbv (shown in Fig. 3), the L1 term is larger than L2. The OH concentrations can be approximately expressed by

$$[HO] = \{J_1[O_3]/(k_1 \times am) \times 2.0 \times k_2[H_2O] + J_2 \times [HONO]\}/ \quad k_3[NO_2] \qquad \text{(R-5)}$$

Where k_3 is the reaction coefficient of $OH + NO_2 \rightarrow HNO_3$.

3. Result and analysis

3.1. OH productions in different HONO conditions

In order to quantify the individual effects of these two OH production terms (P1 and P2) on the OH concentrations, the P1 and P2 are calculated under different daytime HONO conditions (calculated low HONO and measured high HONO concentrations). Figure 8 shows that under the low HONO condition, the P1 is significantly higher than P2, and P2 has only minor contribution to the OH values. For example, the maximum of P1 occurred at 13 pm, with a value of 65×10^6 #/cm^3/s. In contrast, the maximum of P1 occurred at 10 am, with a value of 15×10^6 15 #/cm^3/s. However, under high HONO condition, the P2 plays very important roles for the OH production. The maximum of P1 occurred at 11 am, with a value of 350×10^6 #/cm^3/s, which is about 500% higher than the P1 value. It is important to note that this calculation is based on the high aerosol condition (AOD = 2.5) in September. This result can explain the high O_3 chemical production in Fig. 4.

3.2. OH in different aerosol conditions

In order to understand the effect of aerosol conditions, especially high aerosol conditions, on the OH concentrations. Figure 9 shows the OH concentrations with and without HONO production of OH. With including the HONO production (i.e.,

including P1 and P2), the calculated OH concentrations are significantly higher than without including this production (i.e., only including P1). The both calculated OH concentrations are rapidly changed with different levels of aerosol conditions. For example, without HONO production, the maximum OH concentration is about 7.5×10^5 #/cm^3 under low aerosol condition (AOD=0.25). In contrast, the maximum OH concentration rapidly reduced to 1.5×10^5 #/cm^3 under high aerosol condition (AOD=2.5), and further decreased to 1.0×10^5 #/cm^3 with the AOD value of 3.5. In contrast, with including HONO production, the OH concentrations significantly increased. Under higher aerosol condition (AOD=2.5), the maximum of OH concentration is about 7.5×10^5 #/cm^3, which is the same value under low aerosol condition in the no-HONO case. This result suggests that the measured high O_3 production occurred in the high aerosol condition is likely due to the high HONO concentrations in Shanghai.

3.3. OH in winter

The measurement of O_3 also shows that the concentrations in winter were always low (see Fig. 2), suggesting that the O_3 concentrations were not significantly affected by the appearance of HONO. Figure 10 shows the OH concentrations in September and December. It shows that under different aerosol conditions, OH concentrations in December were very low compared with the values in September. Both the calculated OH concentrations include the HONO production term. For example, under the condition of AOD=2.5, the maximum OH is about 7.5×10^5 #/cm^3 in September, while it rapidly reduces to 1.5×10^5 #/cm^3 in December. Under the condition of AOD=3.5, the maximum OH is still maintaining to a relative high level (4.5×10^5 #/cm^3) in September. However, the maximum OH values are extremely low in December, with maximum value of 0.5×10^5 #/cm^3 in December. Because both the OH chemical productions (P1 and P2) are strongly dependent upon solar radiation (see equation R-4), the seasonal variation of solar radiation plays important roles for controlling the OH production in winter. When the solar radiation is in a very low level in winter, it

reaches a threshold level to prevent the OH chemical production, even by including the HONO production term.

Summary

Currently, China is undergoing a rapid economic development, resulting in a high demand for energy, greater use of fossil fuels. As a result, the high emissions of pollutants produce heavy aerosol pollutions ($PM_{2.5}$) in eastern China, such as in the mega city of Beijing. The long-term measurements show that in addition to the heavy aerosol pollution, the O_3 pollution becomes another major pollutants in the Beijing region. The measured results show that there were very strong seasonal variation in the concentrations of both $PM_{2.5}$ and O_3 in the region. During winter, the seasonal variability of O_3 concentrations were anti-correlated with the $PM_{2.5}$ concentrations. However, during late spring and fall periods, the correlation between $PM_{2.5}$ and O_3 concentrations was positive compared to the negative in winter. This result suggests that during heavy aerosol condition (the solar radiation was depressed), the O_3 chemical production was still high, appearing a double peak of $PM_{2.5}$ and O_3 during fall period. This co-occurrence of high $PM_{2.5}$ and O_3 is the focus of this study. The results are highlighted as follows;

(1) There are high daytime HONO concentrations in major Chinese mega cities, such as in Beijing and Shanghai. It is also interesting to note that the high HONO concentrations were occurred during high aerosol concentration periods. Under the high daytime HONO concentrations, HONO can be photo-dissociated to be OH radicals, and becomes an important process to produce OH.

(2) With including the OH production of measured HONO concentrations, the calculated OH concentrations are significantly higher than without including this production. For example, without HONO production, the maximum OH concentration is about 7.5×10^5 #/cm^3 under low aerosol condition (AOD=0.25),

and rapidly reduced to 1.5×10^5 #/cm^3 under high aerosol condition (AOD=2.5) in September. In contrast, by including HONO production, the OH concentrations significantly increased. For example, under higher aerosol condition (AOD=2.5), the maximum of OH concentration is about 7.5×10^5 #/cm^3, which is similar to the value under low aerosol condition in the no-HONO case. This result suggests that even under the high aerosol conditions, the chemical oxidizing process for O_3 production can be active. This result is likely for explaining the co-occurrence of high $PM_{2.5}$ and high O_3 in fall season in eastern China.

(3) The measurement of O_3 also shows that the concentrations in winter were always low, suggesting that the O_3 concentrations were not significantly affected by the appearance of HONO. The calculated result shows that the seasonal variation of solar radiation plays important roles for controlling the OH production in winter. When the solar radiation is a very low level in winter, it reaches a threshold level to prevent the OH chemical production, even by including the HONO production term.

Because in recent years, the $PM_{2.5}$ pollutions are reduced due to the large control efforts by the Chinese government, the O_3 pollutions become another severe pollution problem in eastern China. This study is important, because it provides some important scientific highlights to better understand the O_3 pollutions in eastern China.

Author contributions. XT came up with the original idea of investigating the scientific issue. XT and JX designed the analysis method. XL, GL and SZ provided the observational data and helped in discussion. XT prepared the manuscript with contributions from all co-authors.

Acknowledgement

This work was supported by the National Natural Science Foundation of China (NSFC) under Grant Nos. 41430424 and 41730108. The Authors thanks the supports of Center for Excellence in Urban Atmospheric Environment, Institute of Urban Environment, Chinese Academy of Sciences. The National Center for Atmospheric

Atmos. Chem. Phys. Discuss., https://doi.org/10.5194/acp-2019-354
Manuscript under review for journal Atmos. Chem. Phys.
Discussion started: 25 April 2019

Research is sponsored by the National Science Foundation.

References

Bian H., S.Q. Han, X. Tie, M.L. Shun, and A.X. Liu, Evidence of Impact of Aerosols on Surface Ozone Concentration: A Case Study in Tianjin, China, *Atmos. Environ*., *41, 4672-4681,* 2007.

Chameides, W. L., Fehsenfeld, F., Rodgers, M. O., Cardelino, C., Martines, J., Parrish, D., Lonneman, W., Lawson, D. R., Ras- mussen, R. A., Zimmerman, P., Greenberg, J., Middleton, P., and Wang, T.: Ozone precursor relationships in the ambient atmo- sphere, *J. Geophys. Res., 97*, 6037–6055, 1992.

Deng X.J, X Tie, D. Wu, XJ Zhou, HB Tan, F. Li, C. Jiang, Long-term trend of visibility and its characterizations in the Pearl River Delta Region (PRD), China, *Atmos. Environ*., *42,* 1424-1435*,* 2008.

Geng, F.H., C.S., Zhao, X. Tang, GL. Lu, and X. Tie, Analysis of ozone and VOCs measured in Shanghai: A case study, *Atmos. Environ*., *41*, 989-1001, 2007.

Geng, FH, CG Cai, X. Tie, Q. Yu, JL An, L. Peng, GQ Zhou, JM Xu, Analysis of VOC emissions using PCA/APCS receptor model at city of Shanghai, China, *J. Atmos. Chem.,* 62, 229–247, DOI :10.1007/s10874-010-9150-5, 2010.

Huang, J.P, X. Y. Liu, C. Y. Li, L. Ding, H. P. Yu, The global oxygen budget and its future projection. *Science Bull. 63,* 1180–1186, 2018.

Huang J., Y. Li, C. Fu, F. Chen, Q. Fu, A. Dai, M. Shinoda, Z. Ma, W. Guo, Z. Li, L. Zhang, Y. Liu, H. Yu, Y. He, Y. Xie, X. Guan , M. Ji, L. Lin, S. Wang, H. Yan and G. Wang, Dryland climate change recent progress and challenges. *Rev. of Geophys., 55,* 719-778, doi:10.1002/2016RG000550, 2017.

Huang, R. J., L. Yang, JJ Cao, QY Wang, X. Tie, et al., Concentration and sources of atmospheric nitrous acid (HONO) at an urban site in Western China. *Sci. of Total Environ*., 593-594, 165-172, doi.org/10.1016/j.scitotenv.2017.02.166, 2017.

Lei, W., R. Zhang, X. Tie, P. Hess, Chemical characterization of ozone formation in the Houston-Galveston area, *J. Geophys. Res., 109,* doi:10.102/2003JD004219, 2004.

Li, G., Bei, N., Cao, J., Wu, J., Long, X., Feng, T., Dai, W., Liu, S., Zhang, Q., and Tie, X.: Widespread and persistent ozone pollution in eastern China during the non-winter season of 2015: observations and source attributions, *Atmos. Chem. Phys., 17*, 2759-2774, doi:10.5194/acp-17-2759-2017, 2017.

Long, X., X. Tie, JJ Cao, RJ Huang, T. Feng, N. Li, SY Zhao, J. Tian, GH Li, Q.

437 Zhang, Impact of crop field burning and mountains on heavy haze in the North
438 China Plain: A case study, *Atmos. Chem. Phys.,* 16, 9675-9691,
439 doi:10.5194/acp-16-9675-2016, 2016.

440 Madronich, S. & Flocke, S. in *Environmental Photochemistry* 2 / 2L, 1–26 (Springer
441 Berlin Heidelberg, 1999)

442 Quan, J.N., Y. Gao, Q. Zhang, X. Tie*, JJ Cao, SQ Han, JW Meng, PF Chen, DL
443 Zhao, Evolution of Planetary Boundary Layer under different weather conditions,
444 and its impact on aerosol concentrations, *Particuology*, doi:
445 10.1016/j.partic.2012.04.005, 2013.

446 Seinfeld, J. H. and Pandis, S. N.: *Atmospheric Chemistry and Physics*: From Air
447 Pollution to Climate Change, 2nd Edn., John Wiley and Sons, New York, 2006.

448 Sillman, S.: The use of NO_y , H_2O_2, and HNO_3 as indicators for
449 ozone-NO_x-hydrocarbon sensitivity in urban locations, J. Geo- phys. Res., 100,
450 14175–14188, 1995.

451 Tie, X., G. Brasseur, C. Zhao, C. Granier, S. Massie, Y. Qin, P.C. Wang, GL Wang,
452 PC, Yang100,, Chemical Characterization of Air Pollution in Eastern China and
453 the Eastern United States, *Atmos. Environ., 40*. 2607-2625, 2006.
454
455 Tie, X., D. Wu, and G. Brasseur, Lung Cancer Mortality and Exposure to
456 Atmospheric Aerosol Particles in Guangzhou, China, *Atmos. Environ*, 43, 2375–
457 2377, 2009a.

458 Tie, X., FH. Geng. L. Peng, W. Gao, and CS. Zhao, Measurement and modeling of O_3
459 variability in Shanghai, China; Application of the WRF-Chem model, *Atmos.*
460 *Environ., 43,* 4289-4302, 2009b.

461 Tie X., F. Geng, A. Guenther, J. Cao, J. Greenberg, R. Zhang, E. Apel, G. Li,
462 A. Weinheimer, J. Chen, and C. Cai, Megacity impacts on regional ozone
463 formation: observations and WRF-Chem modeling for the MIRAGE-Shanghai
464 field campaign, *Atmos. Chem.*
465 *Phys., 13*, 5655-5669, doi:10.5194/acp-13-5655-2013, 2013.

466 Tie, X., Q. Zhang, H. He, JJ Cao, SQ Han, Y. Gao, X. Li, and XC Jia, A budget
467 analysis on the formation of haze in Beijing, *Atmos. Environ*., 25-36, 2015.

468 Tie, X., RJ Huang, WT Dai, JJ Cao, X. Long, XL Su, SY Zhao, QY Wang, GH Li,
469 Effect of heavy haze and aerosol pollution on rice and wheat productions in China,
470 *Sci. Rep.* 6, 29612; doi: 10.1038/srep29612, 2016.

471 Tie, X., J.J. Cao, Understanding Variability of Haze in Eastern China, *J Fundam*

Renewable Energy Appl, 7:6 DOI: 10.4172/2090-4541.100024, 2017.

Tie, X., R.J. Huang, J.J. Cao, Q. Zhang, Y.F. Cheng, H. Su, D. Chang, U. Pöschl, T. Hoffmann, U. Dusek, G. H. Li, D. R. Worsnop, C. D. O'Dowd, Severe Pollution in China Amplified by Atmospheric Moisture, *Sci. Rep.* 7: 15760 | DOI:10.1038/s41598-017-15909-1, 2017.

Zhang, R., X. Tie, and D. Bond, Impacts of Anthropogenic and Natural NO_x Sources over the U.S. on Tropospheric Chemistry, *Proceedings of National Academic Science USA*, *100,* 1505-1509, 2003.

Zhang, Q., C. Zhao, X. Tie, Q. Wei ,G. Li, and C. Li, Characterizations of Aerosols over the Beijing Region: A Case Study of Aircraft Measurements, 40, 4513-4527, *Atmos. Environ.,* 2006.

Atmos. Chem. Phys. Discuss., https://doi.org/10.5194/acp-2019-354
Manuscript under review for journal Atmos. Chem. Phys.
Discussion started: 25 April 2019

Atmospheric Chemistry and Physics Discussions

Figure Caption

Fig. 1. The geographic locations of the measurement sites in Beijing, in which the measured concentrations of $PM_{2.5}$ and O_3 are used to the analysis.

Fig. 2. The daily averaged concentrations of $PM_{2.5}$ and O_3 in the Beijing region in 2015. The concentrations are averaged over all sites shown in Fig. 1. The blue lines represent the $PM_{2.5}$ concentrations ($\mu g/m^3$), and the red bars represent the O_3 concentrations ($\mu g/m^3$). The rectangles show some typical events during winter (green), spring and fall (orange), and summer (red).

Fig. 3. The correlation between O_3 and $PM_{2.5}$ concentrations during winter (upper panel) and during late spring and fall (lower panel). During winter, O_3 concentrations were strong anti-correlated with the $PM_{2.5}$ concentrations. During late spring and fall, O_3 concentrations were correlated with the $PM_{2.5}$ concentrations.

Fig. 4. The diurnal variations of $PM_{2.5}$ (blue line) and O_3 (red line), and NO_2 (green line) during a fall period (from Oct.5 to Oc. 6, 2015). It shows that with high $PM_{2.5}$ condition, there was a strong O3 diurnal variation.

Fig. 5. The effect of aerosol levels with AOD = 0.25 (black line), AOD = 2.5 (red line), AOD = 3.5 (blue line), and AOD = 4.0 (green line) on the O_3 photolysis calculated by the TUV model in October at middle-latitude.

Fig. 6. The measured HONO concentrations (ppbv) in two large cities in China. The red line was measured in Xi'An from 24 July to August 6, 2015. The blue line was measure in Shanghai from 9 to 18 September, 2009. The green line is calculated by the WRF-Chem model. The measurement in fall of Shanghai is applied to the calculation for the OH production of HONO.

Fig. 7. The measured HONO (upper panel) and $PM_{2.5}$ concentrations (lower panel) in fall in Shanghai. It illustrates that the high HONO concentrations were corresponded with high $PM_{2.5}$ concentrations.

Fig. 8. The calculated OH production P(HOx) ($\#/cm^3/s$) by using the model calculated HONO (low concentrations) (in the upper panel) and by using the measured HONO (high concentrations) (in the lower panel). The red bars represent the calculation of the P1 term, and the red bars represent the calculation of the P2 term (OH production from HONO).

Fig. 9. The calculated OH concentrations ($\#/cm^3$) with (upper panel) and without (lower panel) HONO production of OH, under different aerosol levels. Dark red (AOD=0.25), red (AOD=2.5)), red (AOD=3.5)), and red (AOD=4.0).

Atmos. Chem. Phys. Discuss., https://doi.org/10.5194/acp-2019-354
Manuscript under review for journal Atmos. Chem. Phys.
Discussion started: 25 April 2019

Atmospheric Chemistry and Physics Discussions

528 **Fig. 10.** The calculated OH concentrations in September (blue bars) and December
529 (dark red bars), under different aerosol levels.
530
531
532
533

Atmos. Chem. Phys. Discuss., https://doi.org/10.5194/acp-2019-354
Manuscript under review for journal Atmos. Chem. Phys.
Discussion started: 25 April 2019

Atmospheric Chemistry and Physics Discussions

534 # Figures

535

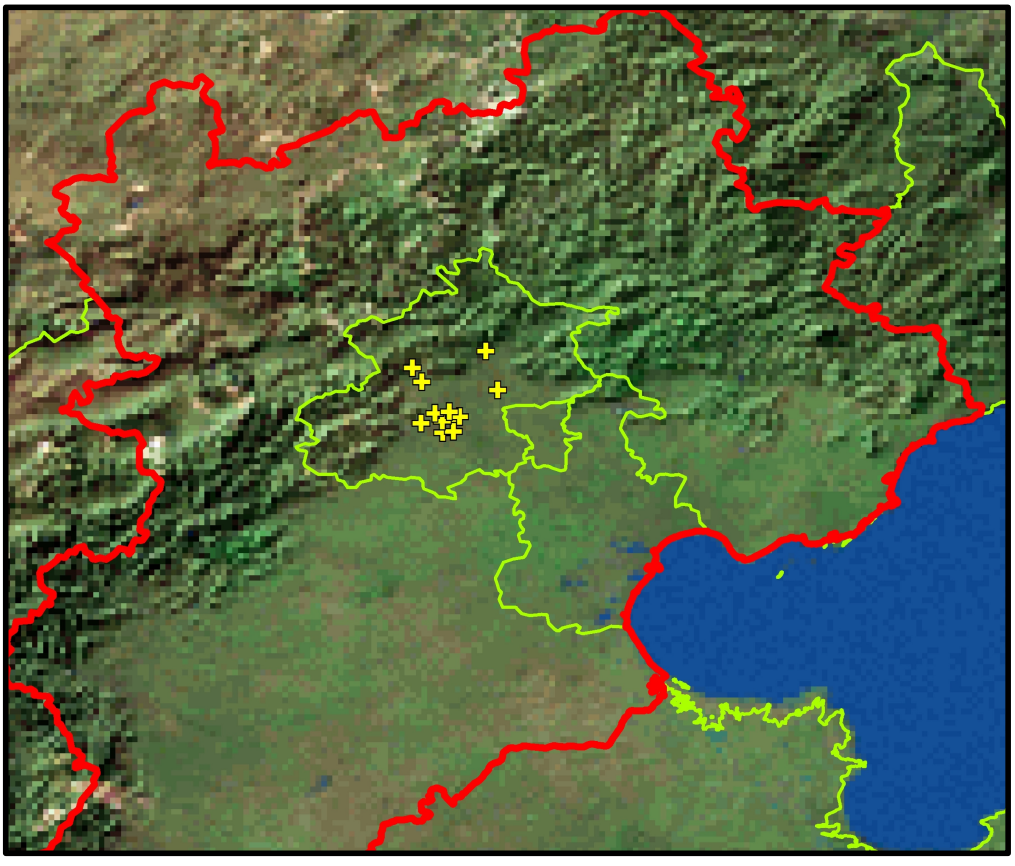

536

537

538 **Fig. 1.** The geographic locations of the measurement sites in Beijing, in which the measured
539 concentrations of $PM_{2.5}$ and O_3 are used to the analysis.

540

Atmos. Chem. Phys. Discuss., https://doi.org/10.5194/acp-2019-354
Manuscript under review for journal Atmos. Chem. Phys.
Discussion started: 25 April 2019

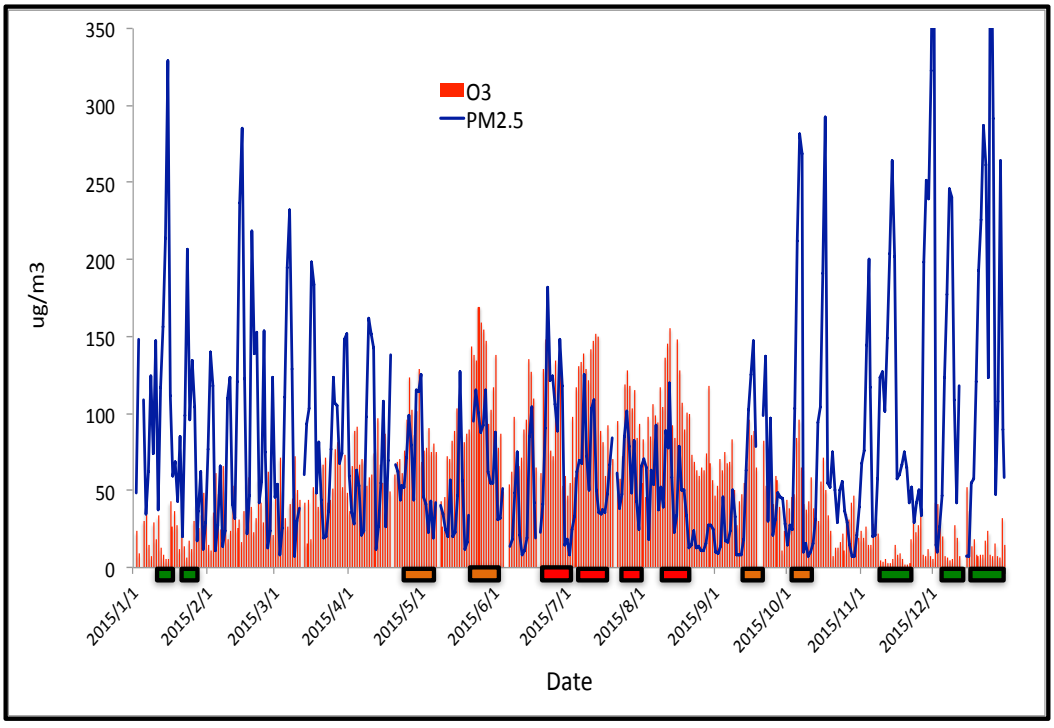

Fig. 2. The daily averaged concentrations of $PM_{2.5}$ and O_3 in the Beijing region in 2015. The concentrations are averaged over all sites shown in Fig. 1. The blue lines represent the $PM_{2.5}$ concentrations ($\mu g/m^3$), and the red bars represent the O_3 concentrations ($\mu g/m^3$). The rectangles show some typical events during winter (green), spring and fall (orange), and summer (red).

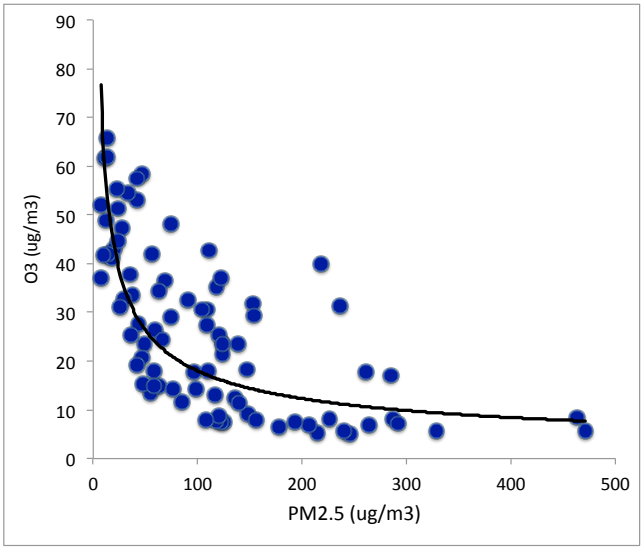

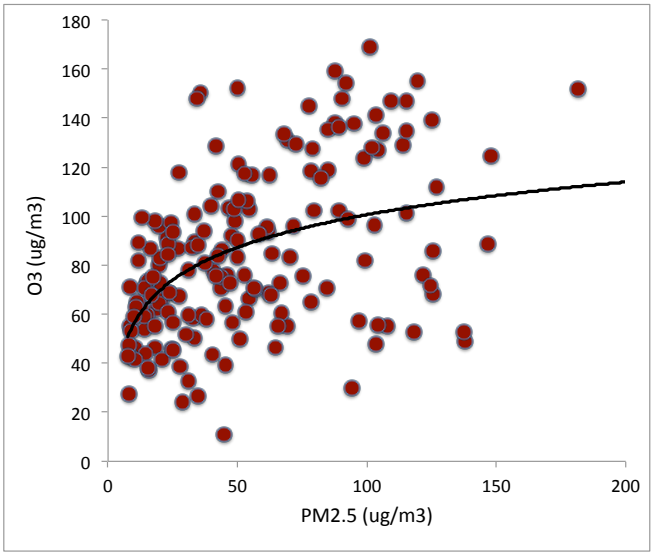

Fig. 3. The correlation between O_3 and $PM_{2.5}$ concentrations during winter (upper panel) and during late spring and fall (lower panel). During winter, O_3 concentrations were strong anti-correlated with the $PM_{2.5}$ concentrations. During late spring and fall, O_3 concentrations were correlated with the $PM_{2.5}$ concentrations.

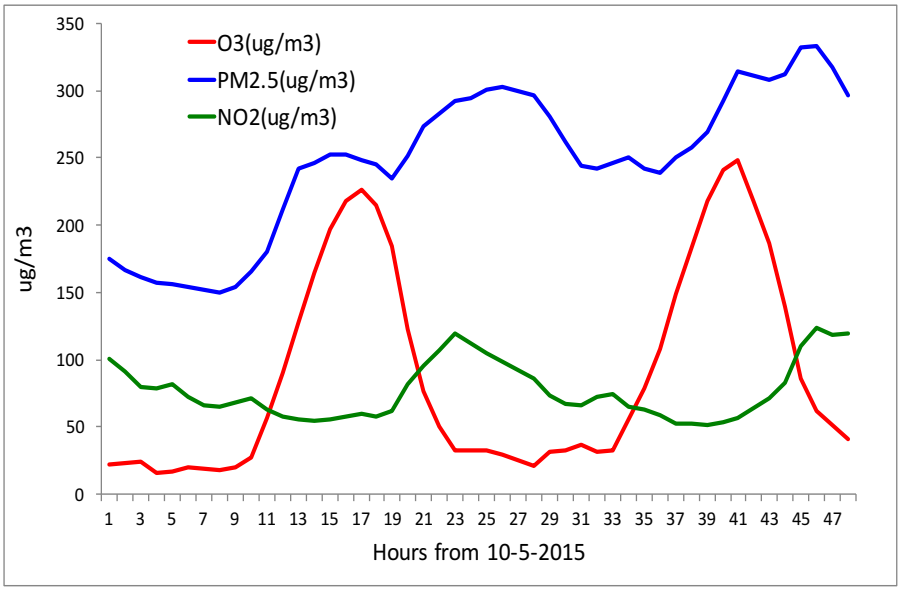

Fig. 4. The diurnal variations of $PM_{2.5}$ (blue line) and O_3 (red line), and NO_2 (green line) during a fall period (from Oct.5 to Oc. 6, 2015). It shows that with high $PM_{2.5}$ condition, there was a strong O3 diurnal variation.

Atmos. Chem. Phys. Discuss., https://doi.org/10.5194/acp-2019-354
Manuscript under review for journal Atmos. Chem. Phys.
Discussion started: 25 April 2019

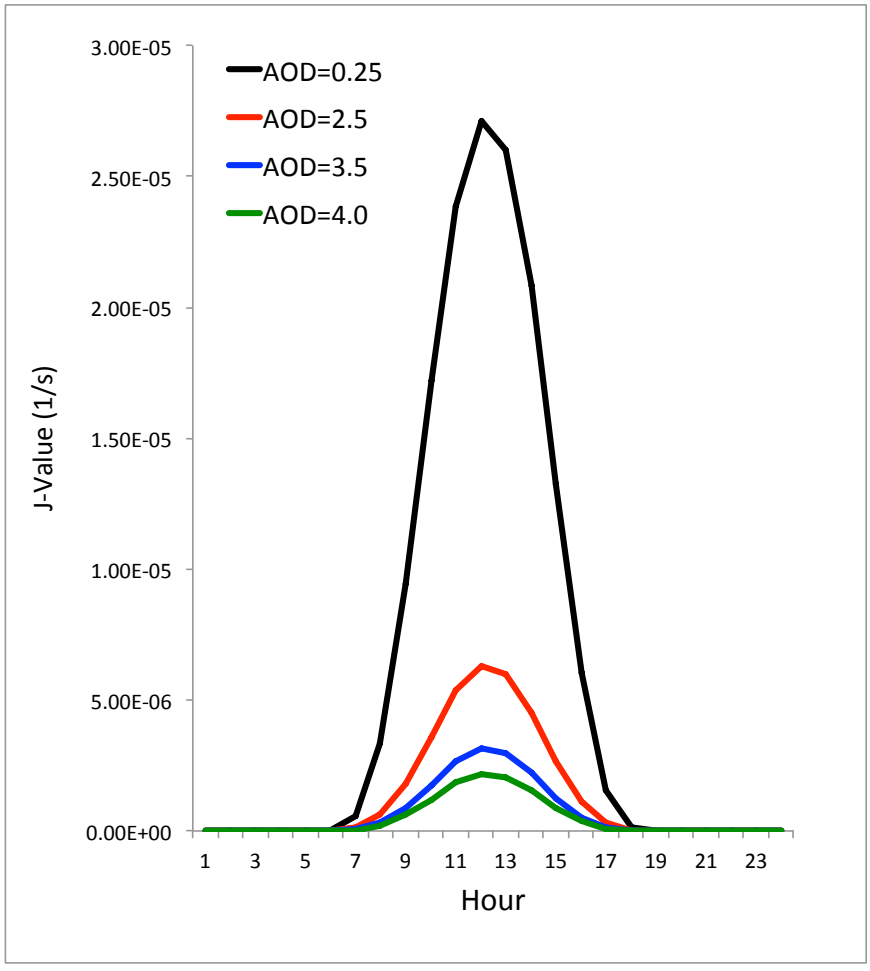

568
569
570 **Fig. 5.** The effect of aerosol levels with AOD = 0.25 (black line), AOD = 2.5 (red line),
571 AOD = 3.5 (blue line), and AOD = 4.0 (green line) on the O_3 photolysis calculated by
572 the TUV model in October at middle-latitude.
573

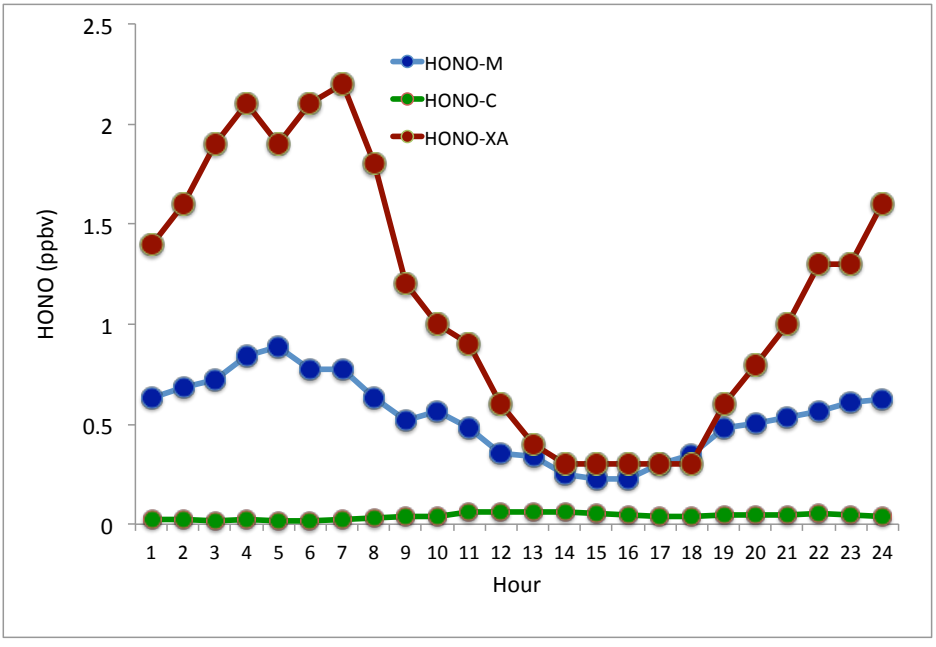

574
575
576
577 **Fig. 6.** The measured HONO concentrations (ppbv) in two large cities in China. The red
578 line was measured in Xi'An from 24 July to August 6, 2015. The blue line was measure
579 in Shanghai from 9 to 18 September, 2009. The green line is calculated by the
580 WRF-Chem model. The measurement in fall of Shanghai is applied to the calculation for
581 the OH production of HONO.

Atmos. Chem. Phys. Discuss., https://doi.org/10.5194/acp-2019-354
Manuscript under review for journal Atmos. Chem. Phys.
Discussion started: 25 April 2019

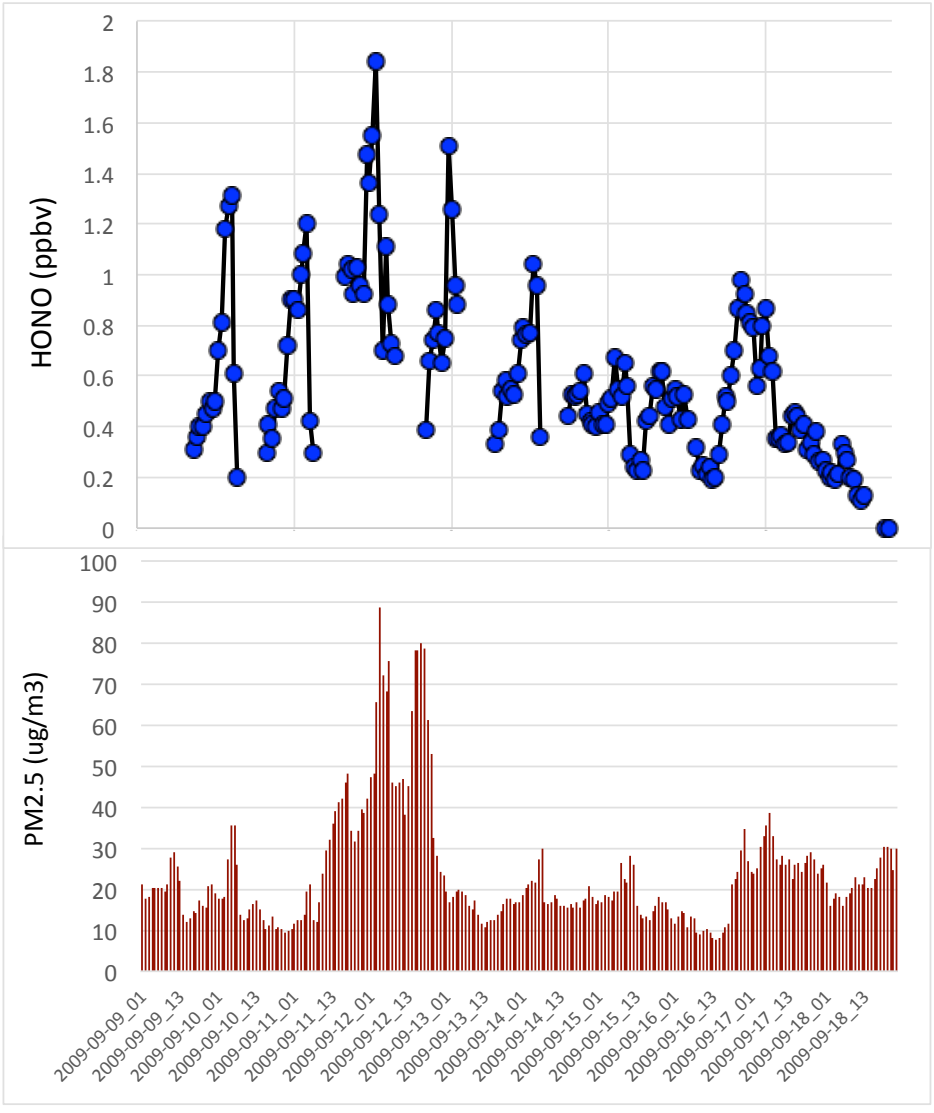

Fig. 7. The measured HONO (upper panel) and $PM_{2.5}$ concentrations (lower panel) in fall in Shanghai. It illustrates that the high HONO concentrations were corresponded with high $PM_{2.5}$ concentrations.

Atmos. Chem. Phys. Discuss., https://doi.org/10.5194/acp-2019-354
Manuscript under review for journal Atmos. Chem. Phys.
Discussion started: 25 April 2019

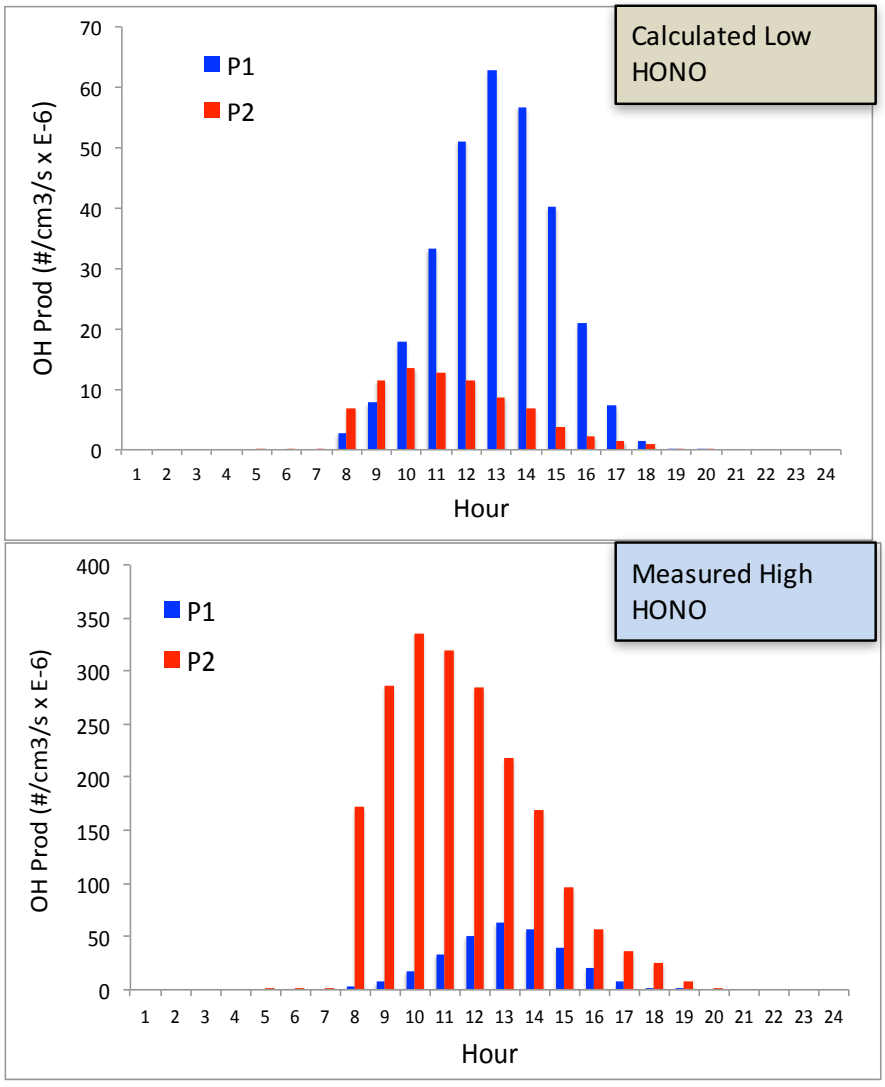

Fig. 8. The calculated OH production P(HOx) (#/cm^3/s) by using the model calculated HONO (low concentrations) (in the upper panel) and by using the measured HONO (high concentrations) (in the lower panel). The red bars represent the calculation of the P1 term, and the red bars represent the calculation of the P2 term (OH production from HONO).

Atmos. Chem. Phys. Discuss., https://doi.org/10.5194/acp-2019-354
Manuscript under review for journal Atmos. Chem. Phys.
Discussion started: 25 April 2019

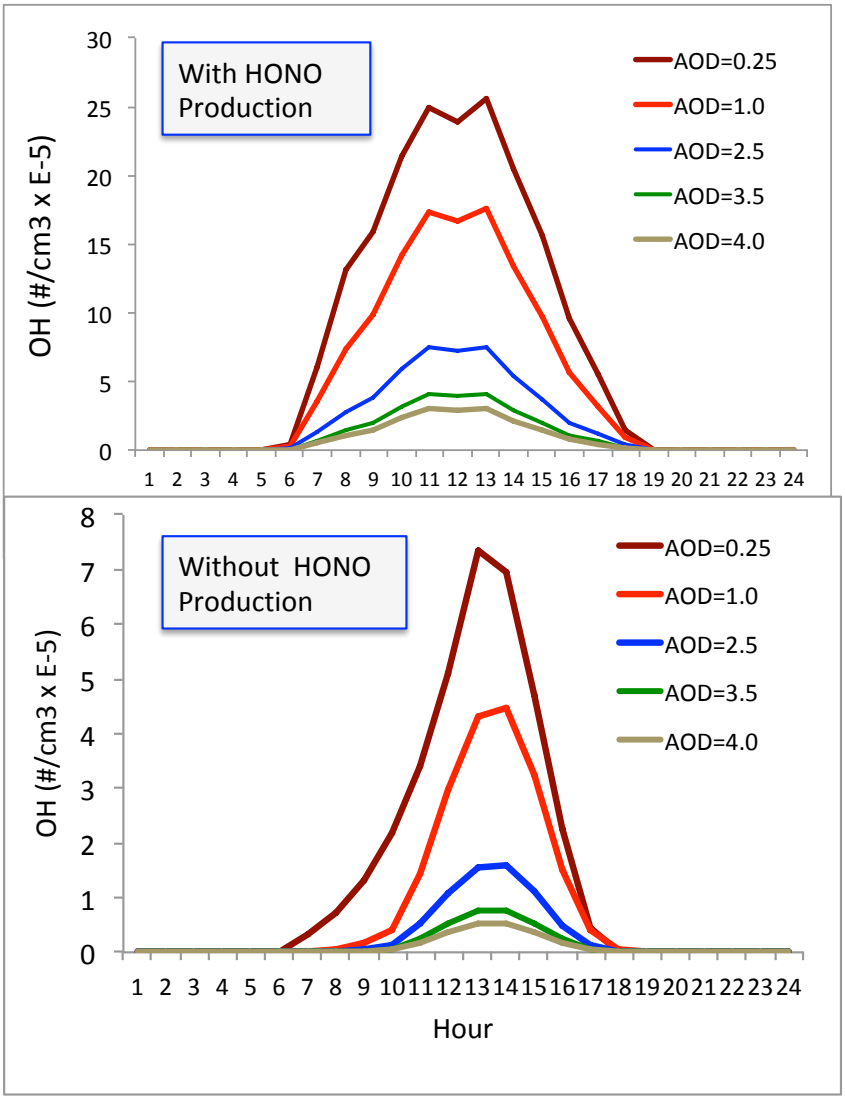

Fig. 9. The calculated OH concentrations (#/cm^3) with (upper panel) and without (lower panel) HONO production of OH, under different aerosol levels. Dark red (AOD=0.25), red (AOD=2.5)), red (AOD=3.5)), and red (AOD=4.0).

Atmos. Chem. Phys. Discuss., https://doi.org/10.5194/acp-2019-354
Manuscript under review for journal Atmos. Chem. Phys.
Discussion started: 25 April 2019

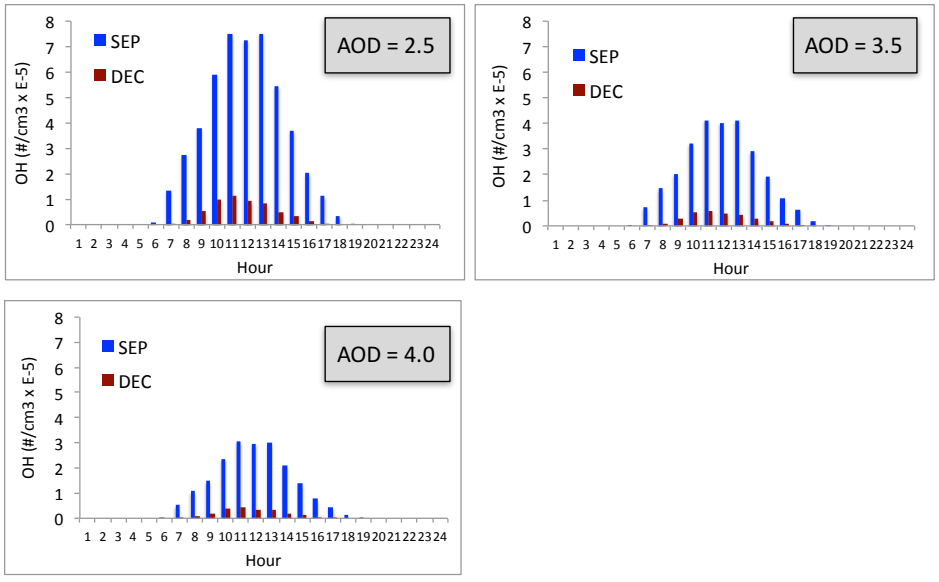

Fig. 10. The calculated OH concentrations in September (blue bars) and December (dark red bars), under different aerosol levels.